AGU PUBLICATIONS

Geochemistry, Geophysics, Geosystems

RESEARCH ARTICLE
10.1002/2017GC006848

Key Points:
- This paper explores changes in the south Pacific helium plume over the period of 1987–2013
- Changes in the plume indicate changes in the mid-depth circulation in the south east Pacific
- Analysis of RAFOS neutrally buoyant drifters from 1987 indicates westward transport at 0.3 cm/s in the plume core

Supporting Information:
- Supporting Information S1
- Table S1

Correspondence to:
J. E. Lupton,
John.E.Lupton@noaa.gov

Citation:
Lupton, J. E., and W. J. Jenkins (2017), Evolution of the south Pacific helium plume over the past three decades, *Geochem. Geophys. Geosyst.*, *18*, 1810–1823, doi:10.1002/2017GC006848.

Received 2 FEB 2017
Accepted 11 MAR 2017
Accepted article online 12 APR 2017
Published online 4 MAY 2017

Evolution of the south Pacific helium plume over the past three decades

J. E. Lupton[1] and W. J. Jenkins[2]

[1]NOAA Pacific Marine Environmental Laboratory, Newport, Oregon, USA, [2]Woods Hole Oceanographic Institution, Woods Hole, Massachusetts, USA

Abstract The recent GEOTRACES Eastern Pacific Zonal Transect in 2013 crossed the East Pacific Rise at 15°S following the same track as the 1987 Helios Expedition along the core of the mid-depth helium plume that spreads westward from the East Pacific Rise (EPR) axis. The fact that several stations were co-located with the earlier Helios stations has allowed a detailed comparison of the changes in the helium plume over the intervening 26 years. While the plume in many areas is unchanged, there is a marked decrease in plume intensity at longitude 120°W in the 2013 data which was not present in 1987. Recent radioisotope measurements along the plume track suggest that this decrease is due to the intrusion of a different water mass into the plume, rather than a modulation of hydrothermal input on the EPR axis. Analysis of GEOTRACES hydrographic data shows excess heat present in the plume up to 0.04°C, corresponding to a ^{3}He/heat ratio of $\sim 2.5 \times 10^{-18}$ mol J^{-1}, similar to that found in mature hydrothermal vents. RAFOS floats deployed in 1987 indicate an average westward transport of $\sim$0.3 cm s^{-1} at 2500 m depth in the off-axis plume, in agreement with recent estimates of $\sim$0.4 cm s^{-1} based on "aging" of the plume from ^{227}Ac/^{3}He ratios.

1. Introduction

During South Tow Expedition in 1972, helium isotope measurements on seven vertical casts spanning the East Pacific Rise (EPR) at latitude 15°S discovered a large plume of ^{3}He-rich water emanating from the EPR crest and extending over 2000 km to the west (see Figure 1) [*Lupton and Craig*, 1981]. The plume was remarkable for several reasons. First, it demonstrated that this portion of the EPR was host to intense hydrothermal sources that were injecting large amounts of ^{3}He into the deep Pacific. Second, the plume showed that helium isotopes were useful for tracking deep ocean circulation and mixing. And finally, the fact that the plume indicated westward flow of mid-depth waters in this region created a controversy, since this westward flow was opposite to that predicted by the Stommel-Arons geostrophic model [*Stommel and Arons*, 1960].

In 1987 a much more detailed survey of the EPR plume was completed during Helios expedition [*Hautala and Riser*, 1993; *Lupton*, 1998]. As part of this survey, samples were analyzed for helium isotopes collected in vertical profiles at 74 separate stations spanning the region from 105°W to 147°W, and 5°S to 20°S. This provided a detailed view of both the longitudinal and meridional extent of the plume (Figure 2). During the two decades after the Helios project, very little work was completed on the off-axis distribution of the EPR plume. One exception was World Ocean Circulation Experiment (WOCE) section P17, which provided a meridional helium section crossing the plume at $\sim$135°W [*Lupton*, 1998; *WOCE*, 2002]. WOCE section P16 also provided helium profiles at the distal end of the plume at 152°W, and NOAA RITS-89 and WOCE P19 provided meridional helium sections at $\sim$105°W and $\sim$88°W, respectively, confirming that the plume is absent to the east of the EPR axis. However, the helium profiles collected during Helios expedition remain the only data set which clearly shows the areal extent of the southern EPR helium plume.

In 2013 the U.S. GEOTRACES Eastern Pacific Zonal Transect collected 35 vertical profiles spanning the EPR at $\sim$15°S [*BCO-DMO*, 2013]. The GEOTRACES track was located to follow the core of the southern EPR helium plume as defined by the previous Helios expedition work. The helium, noble gas, and radiocarbon measurements along the GEOTRACES section are discussed in detail by *Jenkins et al*. [2017]. In addition to helium

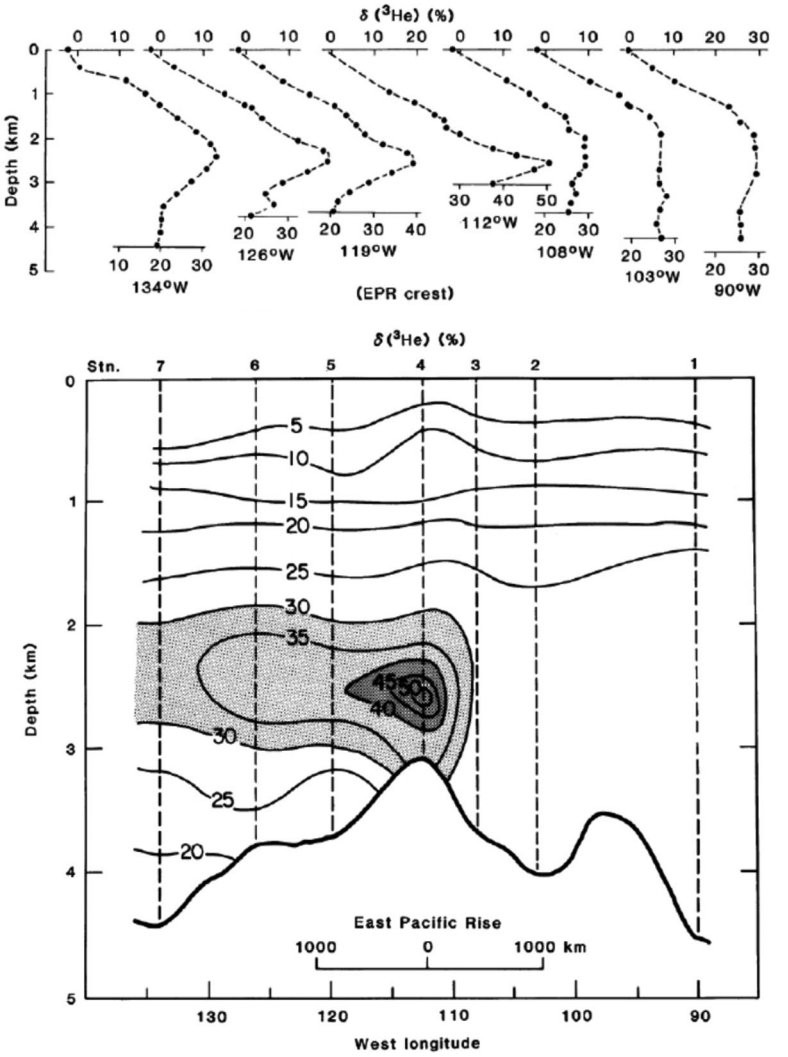

Figure 1. Two figures showing the original discovery of the southern EPR helium plume during South Tow expedition in 1972. Seven vertical profiles were collected spanning the EPR at 15°S [from *Lupton and Craig*, 1981].

isotope measurements, the GEOTRACES Pacific Transect work included measurements of a variety of other tracers, including dissolved Fe, Mn, Al, and Zn, and radioisotopes such as ^{227}Ac, ^{226}Ra, and ^{228}Ra [*Resing et al*., 2015; *Roshan et al*., 2016; *Hammond et al*., 2015; *Kipp et al*., 2016]. In particular, 10 of the GEOTRACES profiles were collected at precisely the same locations as earlier Helios or WOCE helium profiles. This has provided a unique opportunity to investigate temporal variations in the helium plume. In this paper we discuss the evolution of the southern EPR helium plume over the 26 years between 1987 and 2013 by directly comparing the previous Helios helium data with the GEOTRACES results.

2. Historical Views of the Plume

As mentioned in section 1, the 1972 SOTW expedition that crossed the EPR at 15°S revealed the existence of a ^{3}He plume centered at 2500 m depth and extending over 2000 km to the west of the ridge axis (Figure 1). Remarkably, the plume appeared to be absent to the east of the EPR crest, i.e., a profile only 400 km to the east showed background helium values. This strong asymmetry in the plume indicated westward flow at mid-depth in this region, opposite to the eastward flow described in the classic geostrophic circulation model of *Stommel and Arons* [1960]. *Stommel* [1982] suggested that the plume may not be a passive feature, but may in fact be a dynamic feature that seeks to spread westward due to the buoyancy flux of the ascending hydrothermal plumes on the ridge axis. It is clear that the heat flux from hot hydrothermal vents

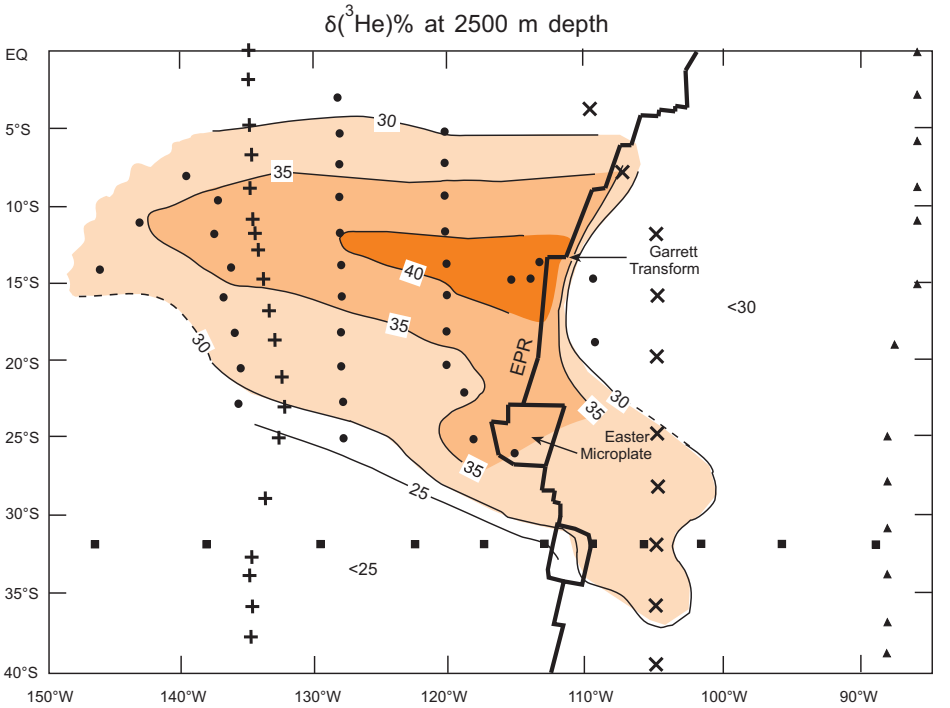

Figure 2. Map of δ^3He (%) contoured on a surface at 2500 m depth for a part of the southeastern Pacific. Contour interval is 5% in δ^3He. The solid black line marks the position of the EPR spreading axis. Helium data are from Helios expedition (solid circles), NOAA RITS-89 (crosses), WOCE P17 (pluses), WOCE P19 (solid triangles), and WOCE P6 (solid squares). All helium measurements made at NOAA/PMEL except WOCE P6, which were measured at WHOI (W. Jenkins, private communication, 1998). Figure taken from *Lupton* [1998].

produces buoyant plumes that entrain and transport ambient deep water several hundred meters vertically in the water column [*Lupton et al.*, 1985; *Lupton*, 1995]. In his model, *Stommel* [1982] theorized that this vertical pumping would result in a dipole source and sink displaced vertically from each other over the ridge axis. According to *Stommel* [1982], in the absence of any background flow, this dipole forcing would then generate a pair of opposing (anticyclonic above cyclonic) zonal gyres extending westward from the EPR axis.

The discovery of the helium plume and the *Stommel* [1982] model generated considerable interest in the plume and the controlling dynamics. *Reid* [1982] showed there is a tongue of salty and warm water coincident with the helium plume extending westward from the EPR axis. This was an expected result, since in the Pacific where salinity increases with depth the rising hydrothermal plumes entrain deeper saltier water and produce a neutrally buoyant plume that is slightly warmer and saltier than the surrounding water [*Lupton et al.*, 1985; *Speer and Rona*, 1989]. Even before the discovery of the helium plume, *Boström et al.* [1969] had generated a map of hydrothermal Mn and Fe recorded in the sediments of the south Pacific extending westward from the EPR very similar to Reid's tongue of warm water. In retrospect the Mn and Fe in the sediments appears to be the "shadow" of hydrothermal particles precipitated from the EPR plume over several decades. *Speer* [1989] expanded on Stommel's work by explicitly including the effects of background flow in a dynamic model. *Thompson and Johnson* [1996] and *Johnson and Talley* [1997] showed that the waters in the core of the off-axis helium plume have a clear θ-S anomaly accompanied by lower stratification (lower N^2), as might be expected from the increased vertical mixing produced in the buoyant plumes on the ridge axis.

In 1987, during Helios expedition, a detailed hydrographic survey was conducted, designed to examine the dynamics of the helium plume. The Helios cruise collected 74 discrete hydrographic profiles, including about 1200 samples analyzed for helium isotopes. Of these, about 33 stations were located off the ridge axis. The Helios samples provided the first detailed map of the lateral extent of the helium plume and showed that the plume maximum actually trends slightly WNW off axis rather than due west (Figure 2). The study confirmed

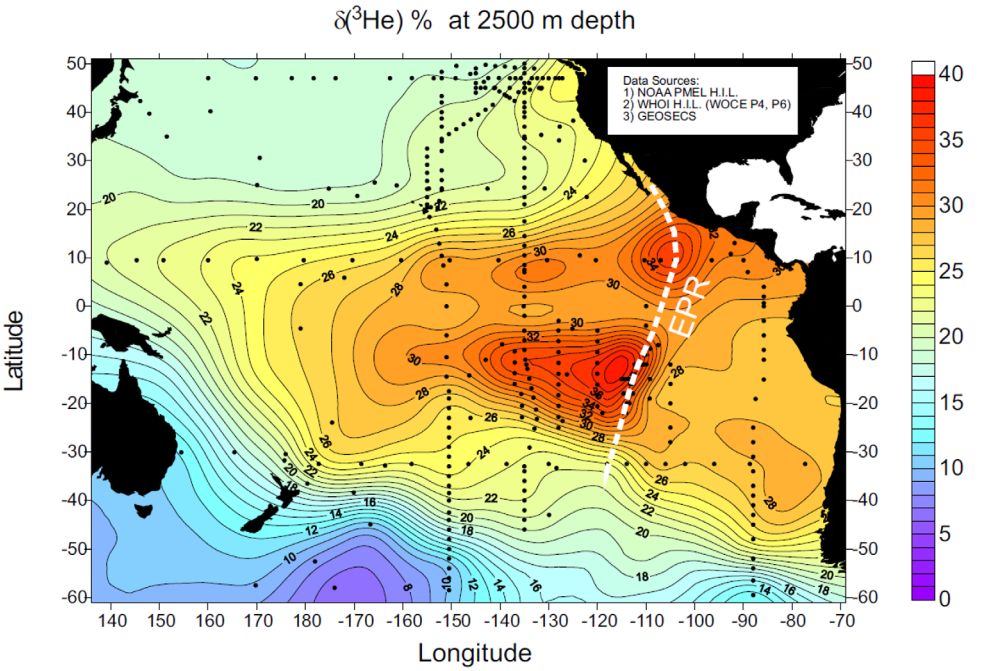

Figure 3. Map of δ^3He (%) for the Pacific Ocean basin contoured on a surface at 2500 m depth. The white dashed line shows the position of the EPR axis. Data from Helios expedition [*Lupton*, 1998] and from WOCE hydrographic program [*WOCE*, 2002]. Note the presence of two major helium jets extending westward from the EPR axis at 10°N and at 15°S.

that the helium signal drops suddenly to background values to the east of the EPR axis at 15°S, and also revealed the presence of a secondary plume trending eastward from the EPR axis at latitude ~30°S.

Several studies have applied inverse modeling to the existing hydrographic data in order to discern the deep flow fields in this region. The geostrophic flow field generated by *Reid* [1981] using steric height analysis is generally consistent with the helium distribution [see *Lupton*, 1998]. *Hautala and Riser* [1993] found that the Helios hydrographic data were consistent with a large-scale circulation driven by a buoyancy flux from the EPR. At plume depth, their β-spiral inverse method found northward flow along the ridge axis, and westward flow in the north, indicating the existence of a large anticyclonic gyre extending >1000 km to the west of the EPR axis. *Faure and Speer* [2012] applied a more detailed inverse method using both hydrographic and tracer data in this region and also found a pattern of anticyclonic recirculation to the west of the EPR. However, all of these inverse methods fail to reproduce the details of the helium distribution, especially the minimum in ^{3}He on the equator (Figure 4).

Subsequent to the Helios expedition, the World Ocean Circulation Experiment and several other projects helped to define the overall helium distribution in the Pacific [*Lupton*, 1998]. Figure 3 shows δ^3He for the entire Pacific contoured on a surface at 2500 m depth. The figure includes Helios data as well as several WOCE sections, including P16, P17, and P19 (along 150°W, 135°W, and 90°W, respectively) and P1, P3, P4, and P6 (along 47°N, 24°N, 9.5°N, and 32.5°S, respectively). Data from NOAA expedition RITS-89 along ~105°W is also included, as well as data from several NOAA expeditions in the northeast Pacific. The figure shows quite clearly that the southern EPR plume is the most significant helium feature in the Pacific, but also reveals a second helium jet extending westward from the EPR axis centered at 10°N. The WOCE P17 section along 135°W (Figure 4) provided a section crossing both of these helium jets, and clearly shows the existence of a minimum in the helium distribution at the equator. A smaller and shallower helium plume is also present in the northeast Pacific due to hydrothermal venting on the smaller Juan de Fuca Ridge [*Lupton*, 1998].

3. RAFOS Floats

In addition to collecting 74 helium profiles, approximately 45 RAFOS neutrally buoyant floats were deployed during the 1987 Helios expedition [see *Rossby et al.*, 1986; *Rossby*, 1991]. The floats were part of an overall

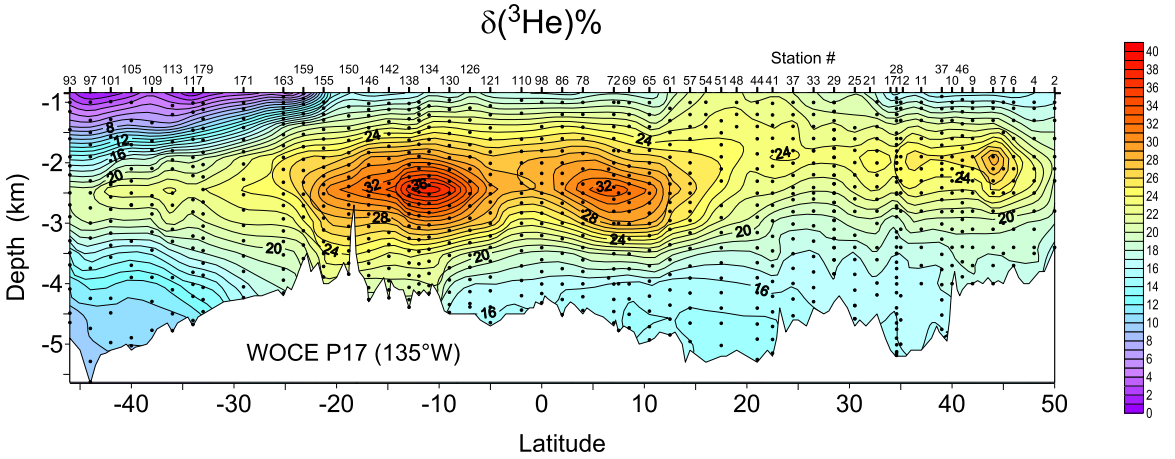

Figure 4. Section view of δ^3He (%) from WOCE P17 along 135°W. Note that this section crosscuts the EPR helium jets at 15°S, 10°N and also the plume emanating from the Juan de Fuca Ridge at ~45°N. Data from the WOCE hydrographic program [*WOCE*, 2002]. Figure from *Lupton* [1998].

study designed to resolve the dynamics of the helium plume [*Hautala and Riser*, 1993]. Of particular interest are the 34 floats that were ballasted to 2500 m depth and deployed either on the rise crest or to the west in the helium plume (Figure 5). The majority of the floats were programmed for a duration of 180 days, and the vectors in the figure indicate the beginning and end points of the each float track. The dashed line indicates the approximate outline of the helium plume.

The float tracks reveal an interesting pattern. The majority of the float tracks in the vicinity of the ridge axis is aligned with the ridge axis itself, possibly confirming the theory that the topography of the ridge tends to divert currents parallel to the ridge axis [*Lavelle*, 2012; *Lavelle et al*., 2012]. The three floats deployed between the equator and 5°S show strong westward transport, possibly indicating entrainment into a near-equatorial jet. As might be expected, the remainder of the float tracks has orientations indicating a strong eddy component. However, the off-axis floats in the core of the plume show a significant average westward transport. The 11 floats deployed off axis in the plume core had an average transport of 0.32 ± 0.13 cm s^{-1} (1-sigma) to the west, and 0.11 ± 0.07 cm s^{-1} (1-sigma) to the north. This corresponds to an average motion of 0.33 ± 0.15 cm s^{-1} WNW along azimuth ~289°. For comparison, the core of the helium plume, based on the Helios map, is oriented approximately along azimuth 280° (Figure 2). The two estimates are consistent in showing a slight northward component. The estimated westward transport of 0.33 cm s^{-1} corresponds to an elapsed time of ~33 years for the hydrothermal helium introduced at the EPR crest to reach the distal end of the plume at longitude 145°W.

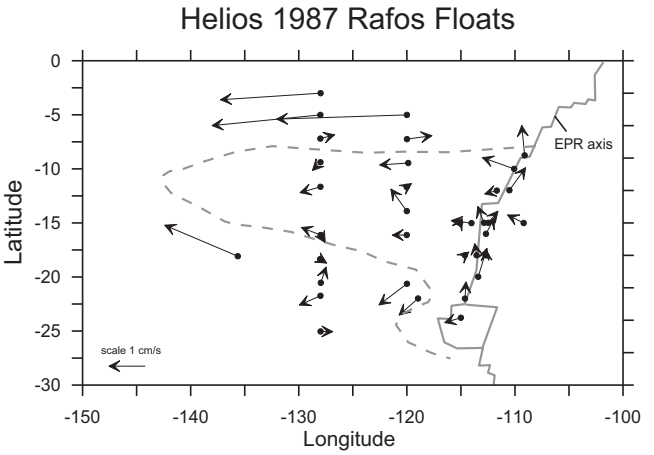

Figure 5. Tracks for the RAFOS neutrally buoyant drifters deployed during the 1987 Helios expedition [see *Rossby et al*., 1986]. The plot shows 18 month tracks for floats at 2500 m depth. The vectors indicate the start and end points for each float, with the scale indicated. The dashed line indicates the outline of the helium plume at δ^3He = 35%. Near the EPR crest the motions are mainly south to north parallel to the ridge axis. In the core of the helium plume off the ridge axis, the floats move west at an average speed of 0.3 cm s^{-1}. This translates to 33 years for the EPR effluent to reach the distal part of the plume at 150°W. Float data from *Rossby* [1991] and *Hautala and Riser* [1993].

Some of the radioisotope measurements made on the GEOTRACES Pacific section samples have provided an interesting comparison with the RAFOS float data. In particular, the longest-lived isotope of actinium, ^{227}Ac ($t_{1/2}$ = 21.77 year), provides the possibility of establishing a time scale for the aging of plume waters. Although most of the ^{227}Ac found in the water column is

derived from the decay of ^{231}Pa in the sediments, *Kipp et al.* [2015] recently showed that there is a separate source of ^{227}Ac from hydrothermal vents. *Hammond et al.* [2015] measured ^{227}Ac in samples along the GEOTRACES Pacific transect and found that the ^{227}Ac/^{3}He ratio in the plume core decreased with distance from the EPR axis indicating an aging of the plume waters going east to west. The rate of decrease in ^{227}Ac/^{3}He corresponded to a horizontal transport of 0.4 cm s^{-1} [*Hammond et al.*, 2015]. Using a similar approach, *Kipp et al.* [2016] used the decrease in the $^{228}Ra_{excess}/^{3}$He ratio in the GEOTRACES data to estimate the spreading rate, and found a westward transport of ~0.1–0.4 cm s^{-1}. Although 26 years have intervened between the RAFOS float experiment and the GEOTRACES section, these estimates of westward transport based on radioisotope measurements are consistent with the 0.3 cm s^{-1} previously estimated from the RAFOS floats. It is notable that the inverse modeling studies of *Hautala and Riser* [1993] and *Faure and Speer* [2012] found similar westward transport velocities of 0.2–0.5 and 0.5 cm s^{-1}, respectively, at the depth of the off-axis plume west of the EPR axis.

3.1. Evolution of the EPR Helium Plume Over the Past 26 Years

As mentioned in section 1, 10 of the GEOTRACES helium profiles were collected at the exact locations where previous Helios, WOCE or RITS-89 profiles were collected in 1987–1989, providing a unique opportunity to examine the time evolution of the helium plume. The positions of these co-located stations are shown in Figure 2. Although the measurements were made on different mass spectrometers in different laboratories at different times (U.C. Santa Barbara versus W.H.O.I), we are confident that the results are comparable, since both laboratories use the same isotopic standard, atmospheric helium. Furthermore, a detailed intercalibration conducted as part of the WOCE helium program demonstrated that the two laboratories agree to better than 0.5% in δ^3He.

Although the profiles were co-located geographically, the samples were not collected at the same water depths. Rather than attempt to interpolate results to common sampling depths, we have instead taken the approach of simply plotting each pair of profiles together. In two cases we have substituted helium results from a different expedition to provide a comparison with the GEOTRACES results where no Helios data were available. We compared 1989 RITS Stn. 18 with GEOTRACES Stn. 15, and we used WOCE P16 Stn. 235 (1991) to compare with GEOTRACES Stn. 36. For the other eight locations we were able to make a direct GEOTRACES versus Helios comparison.

Figure 6 shows plots of δ^3He versus depth for each of the 10 pairs of profiles. At first glance it is apparent that the overall structure of the southern EPR helium plume is unchanged over the intervening 26 years. The profiles at the distal end of the plume at 143°W and 152°W are virtually identical, and the two "background" profiles to the east of the EPR axis at 104°W and 109.2°W also match almost perfectly. The profiles near the EPR axis at 112.75°W, 113.5°W, and 115°W show large differences as might be expected due to changes in the local circulation or variations in the intensity of hydrothermal activity on the EPR crest. However, for each of these near-field profiles the GEOTRACES helium signal is measurably higher than the earlier Helios measurements, possibly indicating an increase in hydrothermal output at 15°S latitude on the EPR axis since 1987.

We also examined changes in the helium plume over time by contouring the 1987 Helios helium data and the GEOTRACES 2013 data using identical gridding parameters. Figure 7 compares the two data sets in section view. Panel C in the figure is a contour of the *difference* between the two grids, which highlights the changes without requiring interpolation to the same sampling depths. It is immediately apparent that there is a minimum in the δ^3He values at about 120°W longitude in the 2013 GEOTRACES section compared to the neighboring stations. This minimum is also present in the GEOTRACES Fe, Mn, and Zn data (Figure 8) [*Resing et al.*, 2015; *Roshan et al.*, 2016]. In contrast, this minimum in the plume is not present in the 1987 Helios section, in which the δ^3He values decrease monotonically westward from the EPR axis (Figure 7). This difference is also apparent in the direct comparison of the two profiles (Figure 6), and even more clearly in Figure 9, which compares the maximum δ^3He for Helios and GEOTRACES versus longitude. The fact that the minimum at 120°W is present in δ^3He, Fe, Mn, and Zn indicates a fundamental change in the plume at that longitude.

3.2. Excess Heat Associated With the Helium Plume

In addition to the helium and trace metals that are introduced by hydrothermal venting, excess heat is also introduced into the water column. In an attempt to detect and characterize this excess heat, we have

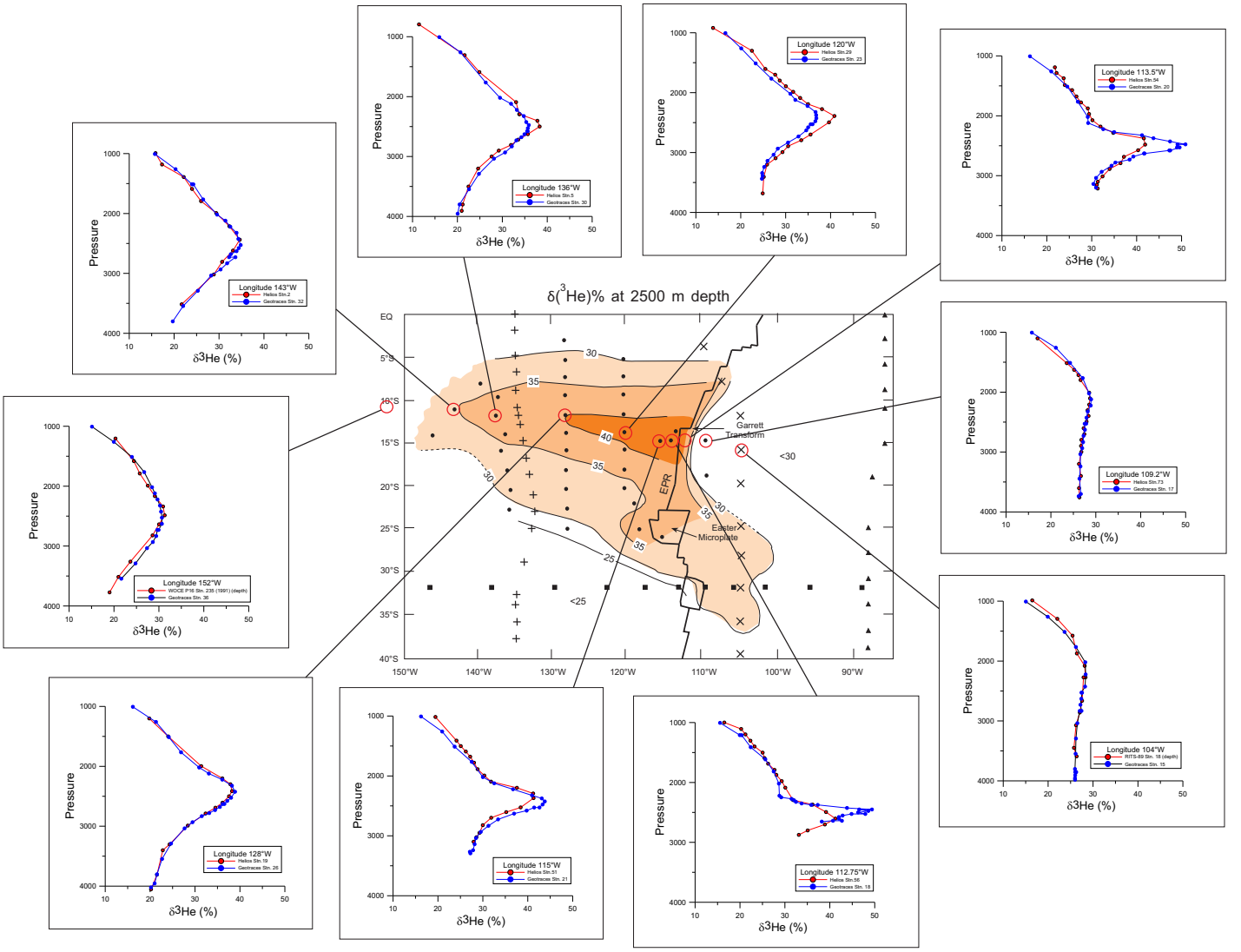

Figure 6. Station by station comparison of 2013 GEOGRACES helium profiles (in blue) versus earlier profiles collected in 1987–1989 (in red) at the same locations. Eight of the earlier profiles are from 1987 Helios expedition. In two cases we substituted profiles from RITS-89 and WOCE P16 to extend the comparison farther west and east along the section.

carefully examined CTD profiles along the GEOTRACES section. Figure 10 shows plots of potential temperature θ, potential density σ, and salinity for two GEOTRACES profiles, one "background" profile to the east of the EPR axis, and another to the west in the core of the helium plume. As shown in Figure 10a, θ versus σ is nearly linear between 2000 and 3200 m for profile G15, east of the EPR axis. The same is true for other "background" profiles east of the EPR axis. Assuming that this linear θ-σ trend is an intrinsic characteristic of background profiles in this region not affected by hydrothermal input, deviations from a linear θ versus σ trend should be a measure of excess heat added to the water column. We have chosen to plot properties versus potential density with the idea that we are then comparing parts of the plume that have ascended to the same neutral density surface.

Figure 10b shows the θ versus σ plot for station G26 at 128°W to the west of the EPR axis. For this station there is a pronounced deviation from linearity as defined by the straight line on the plot, which is a linear fit to the θ, σ values at 2000 and 3200 m depth. The deviation in potential temperature reaches a maximum of ~0.041°C at 2500 m depth for station G26 (see Figure 10e). For comparison, the θ-σ difference for station G15 varies only between −0.005°C to +0.005°C over the entire depth range of 2000–3200 m. As shown in Figure 10c, a plot of θ versus salinity at this station shows an even more pronounced deviation from linearity. This is due to the well-known effect of entrainment and vertical transport of deep saltier water into the

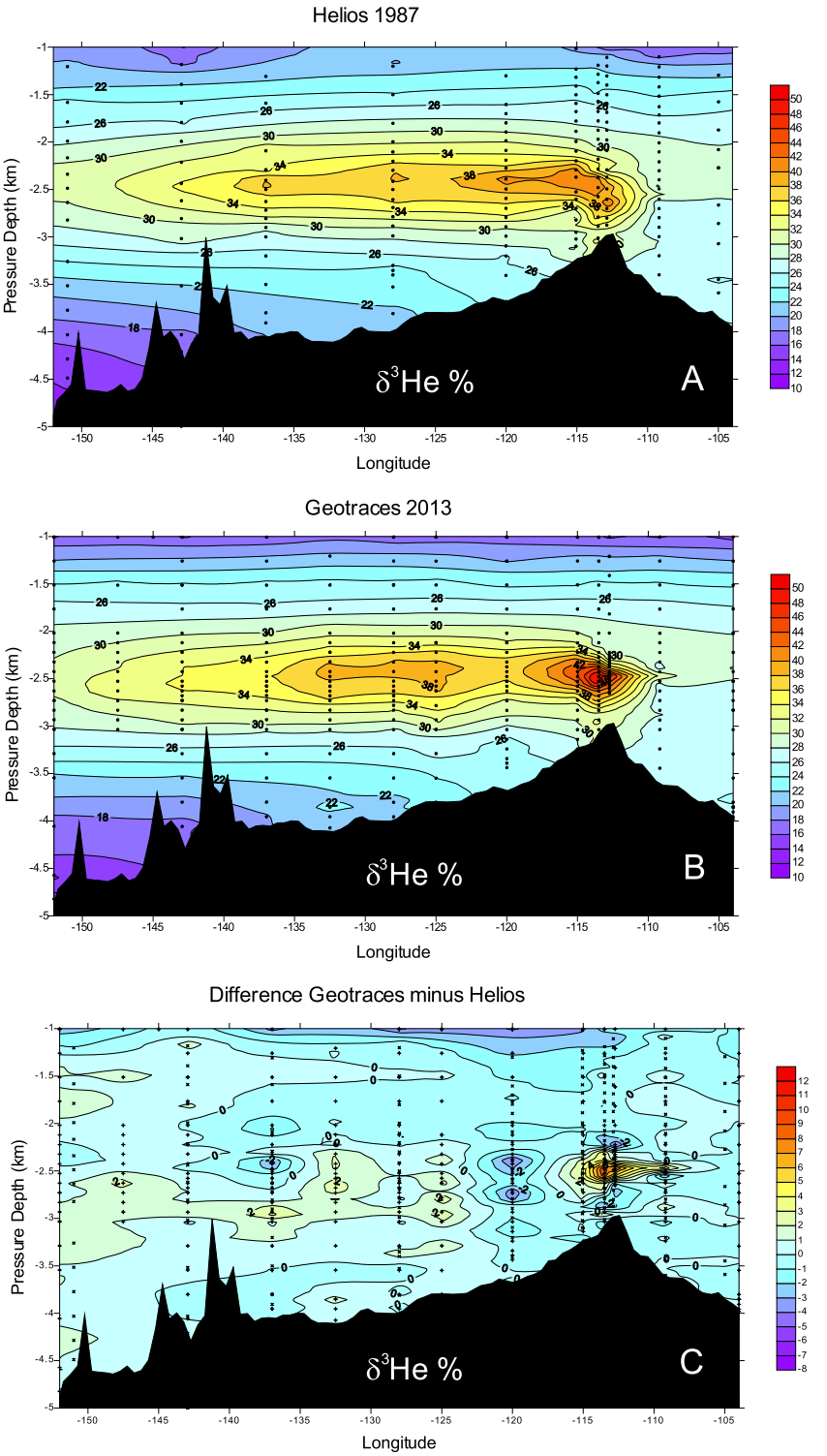

Figure 7. Comparison between the 1987 Helios helium and the 2013 GEOTRACES data contoured in section view using the same gridding parameters. (A) Section view of the 1987 Helios profiles, (B) similar section view of the 2013 GEOTRACES profiles, (C) difference between the two sections created by subtracting the panel A grid from the panel B grid. In general, the differences are small, except over the ridge crest. The other notable difference is that the 2013 GEOTRACES section shows a minimum in the helium signal at 120°W, which is not present in the 1987 Helios data.

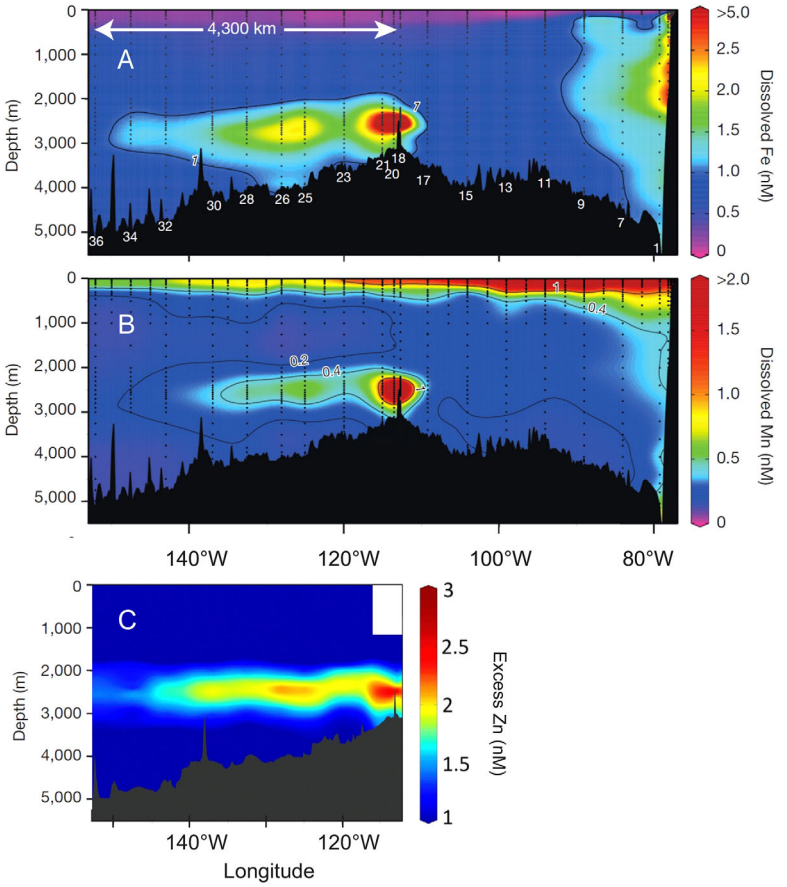

Figure 8. Section plots for dissolved Fe, dissolved Mn, and excess Zn for the 2013 GEOTRACES section [from *Resing et al.*, 2015; *Roshan et al.*, 2016]. These trace metal data mirror the helium data, showing a minimum in the plume signal at 120°W.

rising plume [*Lupton et al.*, 1985]. The presence of this excess salt is clearly evident when salinity is plotted versus potential density (see Figure 10d). Thus, the larger deviation in the θ versus salinity plot includes both the excess temperature component and a "hidden" salinity component added due to entrainment effects. The deviation from linearity in θ versus σ is therefore the most accurate measure of the actual excess heat added to the water column.

Using this approach, we plotted θ versus σ for all 10 GEOTRACES profiles between 104°W and 152°W (not shown). Following the same protocol outlined in Figure 10, we fitted a straight line to the data between 2000 and 3200 m for each station, and then calculated the difference or "θ-σ anomaly" as a function of depth. Our goal was not to provide a perfectly accurate estimate of the excess heat in each profile. However, since we have followed the same protocol for each profile, our results should provide an objective comparison of the different amounts of excess heat present along the GEOTRACES section. For stations G15 and G17 to the east of the EPR axis, the maximum θ-σ anomaly was $<$0.03°C. Beginning with station G18, the θ-σ anomaly for all stations west of the EPR was detectable and reached a maximum at $\sim$2500 m depth, at approximately the same depth as the maximum in ^{3}He (see Figure 10e). Figure 11a shows these results plotted versus longitude for all 10 stations. As might be expected, the θ-σ difference is absent to the east of the EPR, and then makes a sharp jump up to $\sim$0.040°C on the ridge axis. The θ-σ difference for station G23 at 120°W is distinctly lower than that at neighboring stations to the east or west. This confirms that the hydrothermal heat content in the plume at this longitude varies in concert with the concentrations of ^{3}He, Fe, Mn, and Zn, which are all lower than neighboring stations. Unfortunately, the archived Helios CTD data are of poor quality and it was not possible to do a similar analysis of excess heat for the Helios section.

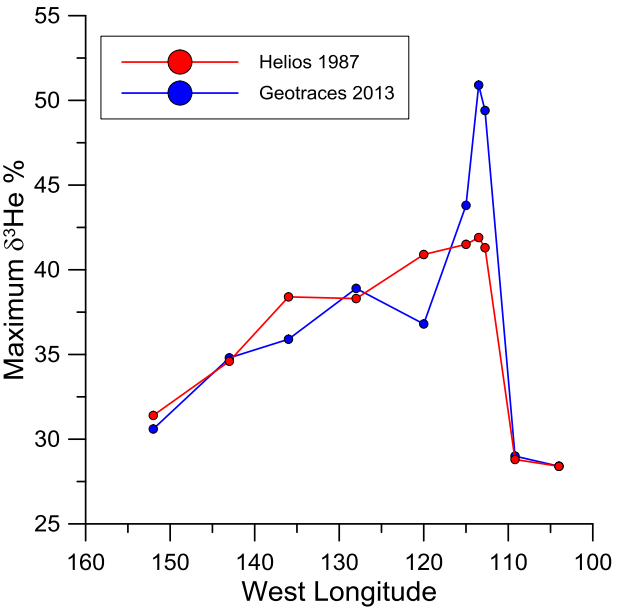

Figure 9. Maximum δ^3He in each profile versus longitude for co-located GEOTRACES 2013 and Helios 1987 stations.

It is also of interest to compare the estimates of excess heat in the plume with the measured ^{3}He concentration. Figure 11b shows the maximum ^{3}He concentration in each of the GEOTRACES profiles plotted versus maximum excess temperature as defined by the θ-σ anomaly. A linear regression fit gives a slope of $\sim 2.5 \times 10^{-18}$ mol J^{-1} for the average ^{3}He/heat ratio in the plume core. The relationship between ^{3}He and heat varies by over an order of magnitude in submarine hydrothermal systems, with systems recently perturbed by magmatic input exhibiting higher ^{3}He/heat and mature long-lived systems having lower ratios [*Lupton et al*., 1999]. Our estimate for the EPR plume is consistent with, although slightly lower than, the typical values of 3 to 4 $\times 10^{-18}$ mol J^{-1} found in long-lived hydrothermal systems [*Lupton et al*., 1999].

There are several reasons to expect that the ^{3}He/heat in the plume cannot be directly compared to that in the hydrothermal fluids. *Lavelle et al*. [1998] showed that the apparent heat anomalies in the water-column plumes underestimate the actual heat released by a factor of 2.1–4.5 for Pacific Ocean waters. This result assumes that the venting fluids have the same salinity as the ambient seawater. *Lavelle et al*. [1998] also showed that this scaling factor is strongly affected when the venting fluids are either saltier or fresher than the ambient seawater, which is often the case. Thus, it is remarkable that our approach for estimating excess heat in the southern EPR plume has produced ^{3}He/heat ratios comparable to typical values measured in hydrothermal fluids.

3.3. Origin of the Plume Minimum at Longitude 120°W

The fact that the minimum at 120°W is present in five different hydrothermal properties measured in the GEOTRACES section (δ^3He, Fe, Mn, Zn, and heat) indicates a fundamental difference in the plume properties at that longitude. It is also quite striking that this minimum in δ^3He is not present in the 1987 Helios section (see Figures 7a and 9), indicating that this feature appeared sometime during the past 26 years. One possibility is that there was a short-term decrease in the rate of helium input feeding the plume in the past. This hiatus in activity would then be carried westward as a minimum in the plume signal. Based on the 0.3 cm s^{-1} westward transport derived from the RAFOS float data, this decrease would have had to have occurred about 7 years ago. Another possibility is that this feature is oceanographic in origin, i.e., it was caused by the intrusion of a different water mass into the plume core rather than a modulation in hydrothermal input.

Some insight into this question is provided by the GEOTRACES radioisotope measurements. As mentioned earlier, *Hammond et al*. [2015] measured ^{227}Ac ($t_{1/2} = 21.77$ year) along the GEOTRACES Pacific transect. They found a local maximum in ^{227}Ac in the plume core at 2500 m depth, indicating a hydrothermal source for the ^{227}Ac at that depth. Second, they found that the ^{227}Ac/^{3}He ratio on $\sigma_\theta = 27.72$ ($\sim$2500 m depth) decreased monotonically from east to west with distance from the EPR axis, providing a "clock" for the aging of the plume, corresponding to a 0.4 cm s^{-1} westward transport [*Hammond et al*., 2015]. Surprisingly, the one exception to this pattern was GEOTRACES Stn. 23 at 120°W, which does not fit the pattern and had much lower ^{227}Ac/^{3}He, indicating the presence of a different water mass at this location, one with an "older" ^{227}Ac/^{3}He age. Similarly, *Kipp et al*. [2016] found lower ^{228}Ra/^{226}Ra and ^{228}Ra/^{3}He at Stn. 23 compared to neighboring stations. These findings point to a mixing or oceanographic origin for this decrease in the plume intensity, since a hiatus in hydrothermal activity on the EPR axis in the past would not be expected to alter the progressive decrease in ^{227}Ac/^{3}He ratios. Thus, it appears that a water mass with lower

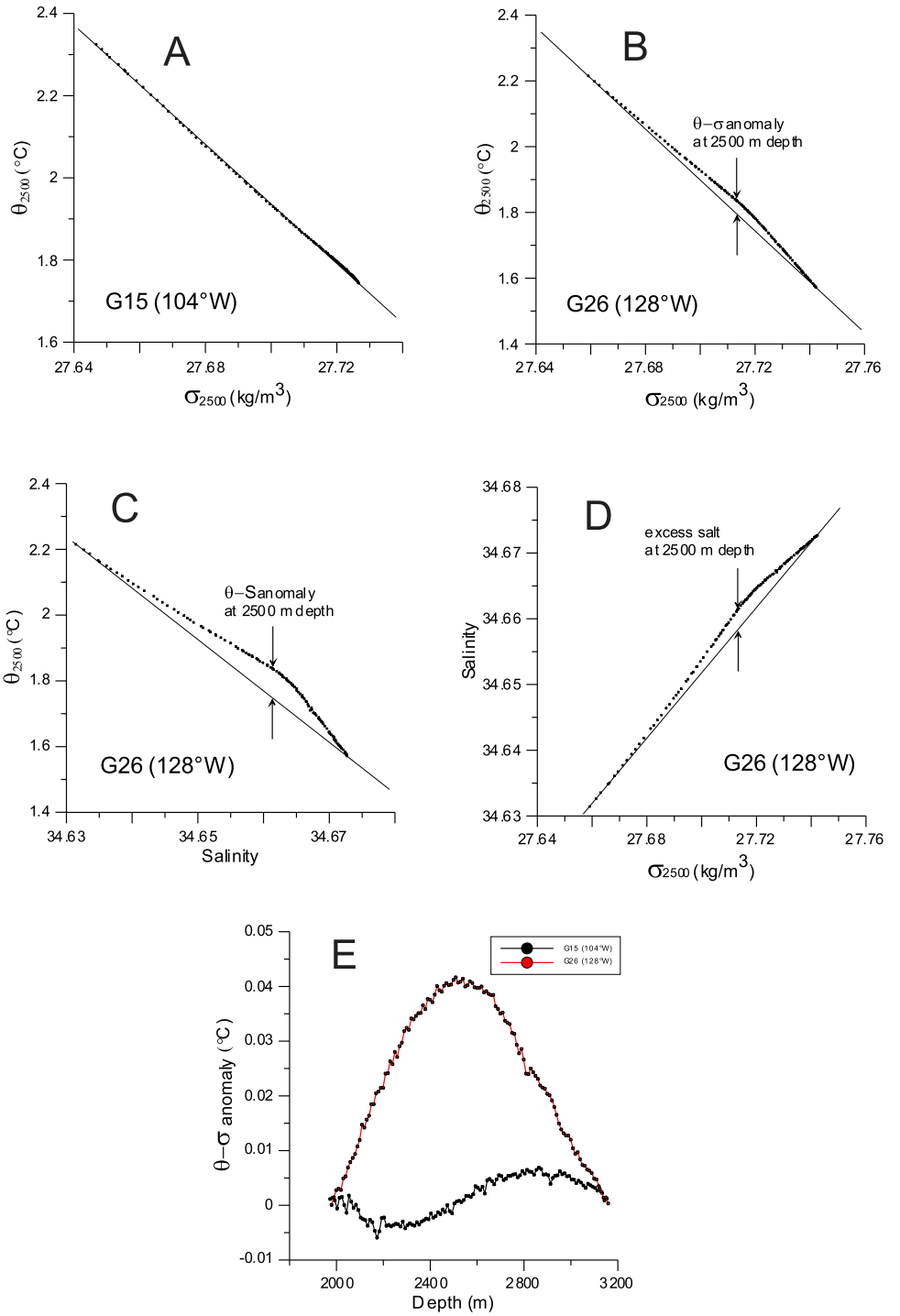

Figure 10. Plots of CTD data between 2000 and 3200 m depth for two GEOTRACES stations. (A) potential temperature θ_{2500} (referenced to 2500 db pressure) versus potential density σ_{2500} (also referenced to 2500 db) for GEOTRACES station G15 located east of the EPR axis, (B) similar plot of θ_{2500} versus σ_{2500} for GEOTRACES station G26 at 128°W west of the EPR axis. The line is a fit between data points at 2000 and 3200 m depth. The θ-σ anomaly is then the difference between the actual data and the fitted straight line. (C) θ_{2500} versus salinity for station G26. (D) Salinity versus σ_{2500} for station G26 showing that there is excess salt in the core of the plume at ~2500 m depth. (E) plots of θ-σ anomaly (°C) versus depth for stations G15 and G26.

concentrations of hydrothermal properties and different radioisotope characteristics intruded into the plume core at this longitude during the intervening 26 years, disrupting the otherwise monotonic changes in plume properties moving east to west.

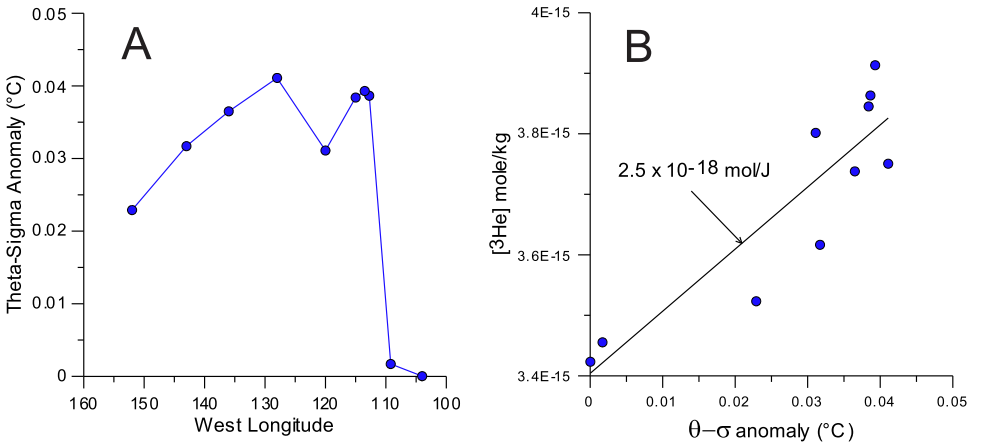

Figure 11. (A) maximum θ-σ anomaly versus longitude for GEOTRACES stations. (B) Maximum ^{3}He concentration versus maximum θ-σ anomaly for the same stations. The line is a linear regression fit to the data, which gives an estimate of the average ^{3}He/heat ratio of 2.5 $\times$ 10^{-18} mol/J.

Jenkins et al. [2017] reached a similar conclusion, namely that the decrease in plume intensity at 120°W is due to mid-depth mixing rather than to modulation of the hydrothermal source. They point out that the lower δ^3He at 120°W is associated with higher Δ^{14}C and lower silica and conclude that the water mass must have come from the south, perhaps as far as 30°S–35°S. This explanation requires the presence of a significant northward mid-depth flow at this longitude spanning 15° in latitude. In contrast to this conclusion, the inverse modeling studies of *Hautala and Riser* [1993] and *Faure and Speer* [2012] both found a broad anticyclonic gyre at plume depth to the west of the EPR with southward transport at 120°W. Thus, an increase in the strength of this gyre circulation could have produced the decrease in plume intensity at 120°W. Furthermore, as shown in Figures 2 and 4, the southern EPR plume is a focused jet in which the plume intensity, as measured by the ^{3}He enrichment, decreases both to the north and south of the plume core. By design the GEOTRACES Pacific transect went down the axis of the 1987 Helios plume. While it is possible that the geographical distribution of the helium plume has changed dramatically since the 1987 Helios survey, this seems unlikely. Thus, it is only necessary to introduce a water mass from a few hundred kilometers north or south of 120°W to produce the observed decrease in δ^3He. Furthermore, there is no indication in the RAFOS float tracks (Figure 5) of a large-scale northward transport at this longitude. We conclude that the change in mid-depth circulation that produced the change at 120°W may have been fairly local, and must have developed in the past few decades, since it was not present in 1987. Note that this conclusion differs from that of *Jenkins et al*. [2017], especially in that the meridional radiocarbon gradient is not consistent with the observed anomaly at 120°W being local.

4. Summary and Conclusions

The GEOTRACES Eastern Pacific Zonal Transect completed in 2013 collected samples down the central axis of the helium plume which spreads westward from the EPR axis at ~15°S. This recent GEOTRACES survey did repeat sampling at several of the Helios expedition stations collected in 1987. We compared 10 GEOTRACES helium profiles with profiles collected ~26 years earlier at the same locations during Helios, RITS-89, and WOCE expeditions. For the most part the helium plume is unchanged over the 26 years. In particular, the profiles at the distal end of the plume at 143°W and 152°W are virtually identical. The GEOTRACES profiles also confirmed that the helium introduced by the hydrothermal venting on the EPR axis is absent to the east of the EPR crest, i.e., the helium signal drops to background values within only a few hundred kilometers to the east of the ridge crest, just as it did in 1987. Thus, at 15°S there is still no tendency for the mid-depth currents to carry the hydrothermal effluent to the east.

While the helium distribution at the eastern and western ends of this EPR transect is relatively unchanged, we detected several differences at other parts of the section. The comparison for profiles at 112.75°W, 113.5°W, and 115°W near the EPR axis show a significant increase in δ^3He compared to the earlier 1987 profiles. One might expect variability in the profiles near the spreading axis due to local oceanographic effects

and to temporal variability in the hydrothermal activity. However, all three of these near-field profiles show an increase in δ^3He, possibly indicating an increase in hydrothermal activity on the EPR at 15°S latitude.

The GEOTRACES section also shows a relative minimum in δ^3He for Stn. 23 at longitude 120°W compared to the neighboring stations, a feature which is also present in other hydrothermal tracers (Fe, Mn, and Zn) measured in the GEOTRACES section. This minimum was not present in the 1987 Helios section, in which δ^3He decreased monotonically from east to west along the section. Analysis of the GEOTRACES temperature and salinity data shows that excess heat up to 0.04°C in the plume associated with hydrothermal input varies in concert with the ^{3}He, also exhibiting a minimum at 120°W. One possible explanation is that there was a decrease or hiatus in hydrothermal activity some time ago which introduced a decrease in δ^3He which has then propagated westward from the EPR crest as a distinct feature imbedded in the plume. The ratio of ^{227}Ac/^{3}He measured at the depth of the δ^3He maximum decreases monotonically westward from the EPR axis, corresponding to "aging" of the plume waters [*Hammond et al*., 2015]. The exception is station 23 at 120°W which has much lower ^{227}Ac/^{3}He than the neighboring stations, indicating that the relative minimum in the plume signal is due to the intrusion of an anomalous water mass at this longitude rather than modulation of the hydrothermal input.

This study has also provided valuable information about the rate at which the mid-depth flow is transporting the EPR effluent westward. In the core of the plume away from the ridge axis, RAFOS neutrally buoyant drifters deployed at 2500 m depth during the 1987 Helios expedition had an average motion of 0.3 cm s^{-1} westward. This is very close to the 0.4 cm s^{-1} westward transport derived 26 years later from the decrease in ^{227}Ac/^{3}He along the GEOTRACES transect [*Hammond et al*., 2015], and is also in agreement with estimates based on radium isotopes [*Kipp et al*., 2016], and inverse modeling studies [*Hautala and Riser*, 1993; *Faure and Speer*, 2012].

This comparison study has confirmed that the southern EPR helium plume is a long-lived feature of the southeastern Pacific driven by westward transport at mid-depth. The plume takes ~30 years to reach its distal end at 150°W, some 4000 km from the ridge axis. In the future, additional hydrographic work and geochemical measurements in the vicinity of 15°S, 120°W would help to clarify the variation in plume intensity detected at that location.

Acknowledgments
We thank Doug Hammond and Lauren Kipp for sharing their unpublished data, and Joe Resing and Saeed Roshan for providing their trace metal data. This paper profited from constructive reviews from D. Hammond and one anonymous reviewer. This work was supported by the Earth Ocean Interactions Program of the NOAA Pacific Marine Environmental Laboratory. This is PMEL publication number 4570.

References

BCO-DMO (2013), U.S. GEOTRACES East Pacific Zonal Transect, Biol. and Chem. Oceanogr. Data Manage. Off., Woods Hole Ocean. Inst., Woods Hole, Mass. [Available at http://www.bco-dmo.org/project/499723.]

Boström, K., M. N. A. Peterson, O. Joensuu, and D. E. Fisher (1969), Aluminum-poor ferromanganoan sediments on active oceanic ridges, *J. Geophys. Res.*, *7*, 3261–3270.

Faure, V., and K. Speer, (2012), Deep circulation in the eastern South Pacific Ocean, *J. Mar. Res.*, *70*, 748–778, doi:10.1357/002224012806290714.

Hammond, D, M. Charette, W. Moore, P. Henderson, V. Sanial, L. Kipp, and R. Anderson (2015), ^{227}Ac in the deep south Pacific along the Peru-Tahiti GEOTRACES transect, paper presented at GEOTRACES Workshop, Santa Catalina, Calif.

Hautala, S. L., and S. C. Riser (1993), A nonconservative β-spiral determination of the deep circulation in the eastern south Pacific, *J. Phys. Oceanogr. 23*, 1975–2000.

Jenkins, W. J., D. E. Lott, C. R. German, K. L. Cahill, J. Goudreau, and B. Longworth (2017), The deep distributions of helium isotopes, radiocarbon, and noble gases along the U.S. GEOGRACES East Pacific Zonal Transect (GP16), *Mar. Chem.*, doi:10.1016/j.marchem.2017.03.009.

Johnson, G. C., and L. D. Talley (1997), Deep tracer and dynamical plumes in the tropical Pacific Ocean, *J. Geophys. Res.*, *102*, 24,953–24,964.

Kipp, L. E., M. A. Charette, D. E. Hammond, and W. E. Moore (2015), Hydrothermal vents: A previously unrecognized source of actinium-227 to the deep ocean, *Mar. Chem. 177*, 583–590.

Kipp, L. E., M. A. Charette, V. S. Sanial, P. B. Henderson, D. E. Hammond, W. S. Moore (2016), Radium isotopes as tracers of hydrothermal inputs and plume dynamics in the deep ocean: Results from Atlantic and pacific US GEOTRACES cruises, presented at the Feb. 2016 Ocean Sciences Meeting, New Orleans, La.

Lavelle, J. W. (2012), On the dynamics of current jets trapped to the flanks of mid-ocean ridges, *J. Geophys. Res.*, *117*, C07002, doi:10.1029/2011JC007627.

Lavelle, J. W., E. T. Baker, and G. J. Massoth (1998), On the calculation of total heat, salt and tracer fluxes from ocean hydrothermal vents, *Deep Sea Res., Part II*, *45*, 2619–2636.

Lavelle, J. W., A. M. Thurnherr, L. S. Mullineaux, D. J. McGillicuddy Jr., and J. R. Ledwell (2012), The prediction, verification, and significance of flank jets at mid-ocean ridges, *Oceanography*, *25*(1), 277–283, doi:10.5670/oceanog.2012.26.

Lupton, J. E. (1995), Hydrothermal plumes: Near and far field, in *Seafloor Hydrothermal Systems: Physical, Chemical, Biological, and Geological Interactions, Geophys. Monogr. Ser.*, vol. 91, edited by S. E. Humphris et al., pp. 317–346, AGU, Washington, D. C.

Lupton, J. E. (1998), Hydrothermal helium plumes in the Pacific Ocean, *J. Geophys. Res.*, *103*, 15,853–15,868.

Lupton, J. E., and H. Craig (1981), A major ^{3}He source on the East Pacific Rise, *Science*, *21*, 13–18.

Lupton, J. E., J. R. Delaney, H. P. Johnson, and M. K. Tivey (1985), Entrainment and vertical transport of deep-ocean water by buoyant hydrothermal plumes, *Nature*, *316*, 621–623.

Lupton, J., E. T. Baker, and G. J. Massoth (1999), Helium, heat, and the generation of hydrothermal event plumes at mid-ocean ridges, *Earth Planet. Sci. Lett.*, *171*, 343–350.

Reid, J. L. (1981), On the mid-depth circulation of the world ocean, in *Evolution of Physical Oceanography*, edited by B. A. Warren and C. Wunsch, pp. 70–111, MIT Press, Cambridge, Mass.

Reid, J. L. (1982), Evidence of an effect of heat flux from the East Pacific Rise upon the characteristics of the mid-depth waters, *Geophys. Res. Lett.*, *9*, 381–384.

Resing, J. A., P. N. Sedwick, C. R. German, W. J. Jenkins, J. W. Moffett, B. M. Sohst, and A. Tagliabue (2015), Basin-scale transport of hydrothermal dissolved metals across the South Pacific Ocean, *Nature*, *523*, 200–203, doi:10.1038/nature14577.

Rossby, H. T. (1991), Large scale circulation in the area of the East Pacific Rise and the helium-3 plume, Abstract presented at 2nd Annual Meeting, The Oceanogr. Soc., St. Petersberg, Fla.

Rossby, T., D. Dorson, and G. Fontaine (1986), The RAFOS system, *J. Atmos. Oceanic Technol.*, *3*, 672–680.

Roshan, S., J. Wu, and W. J. Jenkins (2016), Long-range transport of hydrothermal dissolved Zn in the tropical South Pacific, *Mar. Chem.*, *183*, 25–32, doi:10.1016/j.marchem.2016.05.005.

Speer, K. G. (1989), The Stommel and Arons model and geothermal heating in the South Pacific, *Earth Planet. Sci. Lett.*, *95*, 359–366.

Speer, K. G., and P. A. Rona (1989), A model of an Atlantic and Pacific hydrothermal plume, *J. Geophys. Res.*, *94*, 6213–6220.

Stommel, H. (1982), Is the south Pacific helium-3 plume dynamically active?, *Earth Planet. Sci. Lett.*, *61*, 63–67.

Stommel, H., and A. B. Arons (1960), On the abyssal circulation of the world ocean, II, An idealized model of circulation pattern and amplitude in oceanic basins, *Deep Sea Res.*, *6*, 217–233.

Thompson, L., and G. C. Johnson (1996), Abyssal currents generated by diffusion and geothermal heating over rises, *Deep Sea Res., Part I*, *43*(2), 193–211.

WOCE (2002), World Ocean Circulation Experiment, Natl. Centers for Environmental Information (ncei.noaa.gov), formerly Natl. Oceanogr. Data Center. [Available at https://www.nodc.noaa.gov/woce/.]